OPTIMIZATION AND EVALUATION IN SPACE CONDITIONS OF MULTI-GHZ OPTICAL MODULATORS

Henri Porte[1], Arnaud Le Kernec[2], Laura Peñate Quesada[3], Ignacio Esquivias[4], Houda Brahimi[1], Juan Barbero Gonzalez[3], Alexandre Mottet[1], Michel Sotom[2]

[1]*Photline Technologies, 16 rue Jouchoux, 25000 Besançon France,*
[2] *Thales Alenia Space, 26, av. J-F. Champollion - BP 1187, 31037 Toulouse Cedex 1 ,*
[3]*Alter Technology TÜV NORD S.A.U. C/ La Majada 3. 28760 Tres Cantos - Madrid (SPAIN),*
[4]*Universidad Politécnica de Madrid, CEMDATIC-E.T.S.I. Telecomunicación Ciudad Universitaria, 28040 Madrid, Spain*

I. INTRODUCTION

Among the different optical modulator technologies available such as polymer, III-V semiconductors, Silicon, the well-known Lithium Niobate (LN) offers the best trade-off in terms of performances, ease of use, and power handling capability [1-9]. The LN technology is still widely deployed within the current high data rate fibre optic communications networks. This technology is also the most mature and guarantees the reliability which is required for space applications [9].In or der to fulfil the target specifications of opto-microwave payloads, an optimization of the design of a Mach-Zehnder (MZ) modulator working at the 1500nm telecom wavelength was performed in the frame of the ESA-ARTES "Multi GigaHertz Optical Modulator" (MGOM) project in order to reach ultra-low optical insertion loss and low effective driving voltage in the Ka band. The selected modulator configuration was the X-cut crystal orientation, associated to high stability Titanium in-diffusion process for the optical waveguide. Starting from an initial modulator configuration exhibiting 9 V drive voltage @ 30 GHz, a complete redesign of the coplanar microwave electrodes was carried out in order to reach a 6 V drive voltage @ 30GHz version. This redesign was associated to an optimization of the interaction between the optical waveguide and the electrodes.

Following the optimisation steps, an evaluation program was applied on a lot of 8 identical modulators. A full characterisation was carried out to compare performances, showing small variations between the initial and final functional characteristics. In parallel, two similar modulators were submitted to both gamma (10-100 krad) and proton irradiation (10.10^9 p/cm²) with minor performance degradation.

II. OPTICAL MODULATOR APPLICATIONS AND REQUIREMENTS

During past years, innovative payload concepts based on photonic technologies were investigated by Thales Alenia Space [10-11]. Several architectures were elaborated covering different application cases including (but not limited to) flexible analogue repeaters based on a photonic centre section and photonic receiver front-ends for advanced antennas allowing digital beam forming. Such architectures rely on photonic subsystems able to assist, complement, replace and/or extend the capabilities of conventional RF subsystems including:

- Optical generation/distribution of microwave Local Oscillators (LO)
- Photonic RF frequency up and down conversion
- Routing of µ-wave signals in repeaters
- Photonically assisted beam forming networks
- Optical sampling for analogue to digital conversion

In this context, optical modulators play a key role in the implementation of such functions.

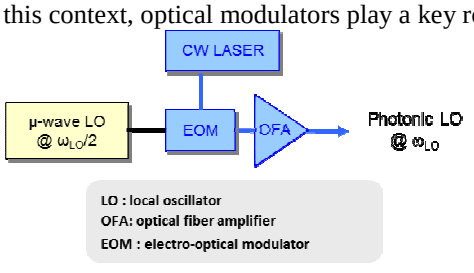

Fig. 1. Microwave photonic Local Oscillator (LO) based on DSB-CS Schematic

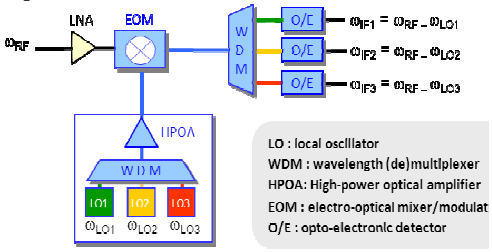

Fig. 2. Optical Multi-Frequency Conversion concept

For instance, the optical distribution of LO's requires to produce a microwave LO signal, under optical form, with low phase noise and optical power high enough to be deliveredto a large number of receivers while meeting system requirements. The transfer of a high-frequency signal onto an optical carrier through direct modulation of the laser current is not applicable at high frequencies and requiresexternal electro-optical intensity modulators. In particular, optical double sideband modulation with carrier suppression (DSB-CS) is a LO generation technique making use of a high-power CW laser and a MZ electro-optical modulator (EOM) biased at minimum optical transmission, as shown in Figure 1. When the modulator is driven by a microwave signal at $\omega_{LO}/2$ frequency, the optical output signal mainly contains the first two modulation side-bands. Optical heterodyning at the photo receiver generates a microwave signal at the ω_{LO} frequency.

Photonic RF frequency mixing for both up and down conversion of microwave signals can be achieved optically by means of EOMs. The sinusoidal transfer function of MZ modulators make them attractive as mixers. In addition to a very wide bandwidth and an infinite LO to RF input port isolation, a remarkable feature of electro-optical mixing is its ability to perform simultaneously multiple frequency-conversions. In this concept, shown in Figure 2, the optical mixer is fed by several optical LO's through wavelength-division-multiplexing (WDM). In this way, the RF signal at the ω_{RF} frequency driving the modulator is mixed to the different LO's and frequency-converted to several signals at various ω_{IF} frequencies. The most critical requirements for the EOM in previously depicted applications are low optical loss, high dynamic extinction ratio, high optical power handling capability and low RF half-wave voltage. . More exhaustively, an efficient optical modulator shall, in particular:

- operate in the high frequency domain (to comply with Ka band requirements and above),
- operate under low driving power (to lower the power consumption budget of the overall system)
- exhibit low optical insertion loss (to improve RF gain and noise figure performance),
- handle high optical input power (to improve RF gain and noise figure performance),
- feature good linearity (to meet the requirements of analogue systems),
- come in small size (to accommodate in systems where size is critical, e.g. phased array antennas),
- withstand the space environment constraints.

The Table 1 hereafter summarizes typical specifications for optical intensity modulators used in these applications.

ITEM	TARGET FIGURE
Operating wavelength	1520 – 1600 nm
Maximum input optical power handling	200 mW
Optical insertion loss	≤ 3 dB
RF operating frequency	Up to 40 GHz
RF driving voltage (or power) @ 30 GHz (Note 1)	≤ 4 V (≤ +16 dBm)
Dynamic extinction ratio	≥ 20 dB
Linearity : carrier-to-3rd intermodulation (Note 2)	≥ 60 dBc
Impedance	50 ohms
RF return loss (in the band)	≥ 15 dB
Optical fibre input/output	PMF / PMF or SMF (Note 3)
Package	hermetic
Volume	≤ 8 cm^3
Mass	≤ 20 g
Lifetime	≥ 15 years

(Note 1) Peak-to-peak RF voltage (or power) for 100% modulation at 30 GHz, i.e. half-wave voltage for Mach-Zehnder modulator.
(Note 2) Carrier-to-Intermodulation ratio, with 2-tone @ 30 GHz, and power per tone 25 dB below RF drive power
(Note 3) Polarisation-maintaining fibre / Polarisation-maintaining fibre or Single-mode fibre

Table 1 : Typical modulator specifications

It is practical in microwave analogue applications to use the following figure of merit (FoM) :

$$FoM = \left[\frac{10^{-\frac{\alpha_{dB}}{10}}}{V_{\pi RF}} \right]^2 \quad (1)$$

Where α_{dB} is the optical insertion loss (dB), and $V_{\pi RF}$ is the effective half-wave voltage (V) at the operating frequency. One should notice that the RF gain of a non-amplified link is directly proportional to this FoM, and that the RF noise figure is inversely proportional to this FoM. The factor of merit described here will be a guideline in the following description. We describe in the next paragraphs the MZ modulator.

III. NEW MODULATOR DESIGN

A previous assessment of different modulator technologies highlighted the suitability of LN modulator as a mature and promising technology for space applications [9].

Figure 3 shows a conventional broadband modulator. It is constructed from a Mach-Zehnder waveguide integrated in a LN substrate. Depending on the aimed performances, two crystals orientations are possible. In many cases, for thermal stability reasons, the crystal orientation is X-cut.The reason is that the Z-cut orientation is sensitive to pyroelectric effects requiring thus special antistatic layers in the fabrication to avoid failures due to temperature variations. Single drive Z-cut modulators are also characterized by chirp which can be a drawback for DSB-CS modulation.

Two technologies can be used for the waveguide fabrication. However, the technology called Titanium in-diffusion waveguide (TI-WG) is preferred to proton exchange for thermal stability reasons. For an amplitude or intensity modulator, the design of a waveguide is the Mach-Zehnder configuration with one input waveguide, a Y-branch section for spatial separation of the input beam in two waves, two parallel waveguide arms, a second Y-branch section and an output waveguide playing the role of modal filter.

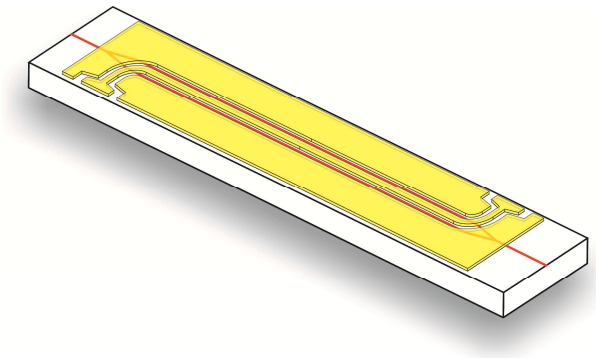

Fig. 3. Microwave electro-optic Mach-Zehnder modulator

Coplanar waveguide microwave electrodes are patterned in order to allow the electro-optic interaction between the electric signal and the optical light field propagating into the waveguide. A silica buffer layer is introduced between the electrodes and the waveguide in order to achieve the 50 Ω characteristic impedance. The thickness of the buffer is selected in order to reach the phase matching condition, i.e. the microwave effective index is equal or very close to the optical effective index. Moreover, the thickness of the gold electrodes is adjusted in order to reduce the conductor loss. Finally, the gap between the central line and the lateral ground plane is designed to optimize the driving voltage.

In order to reach the targeted performances required in microwave photonic payloads, described in section I, it was necesary to improve the initial version of the Photline broadband analog modulator. This initial version exhibited a half-wave voltage in excess of 9 V at 30 GHz and the RF and DC electrodes were separated. Following multiple microwave and optical simulations, a new version was designed. One single RF electrode allowed driving both the RF and DC voltage via a dedicated bias tee termination. The CPW electrodes and optical waveguide designs were deeply remodeled in order to ensure an effective driving voltage reduced by

30% while keeping a minimal footprint. The housing was also improved in order to reach a smaller form factor (85 mm long packaging while previous version was 100 mm long).

To validate the new modulator design, prototypes were submitted to a functional test campaign and thermal tests were carried out to assess their stability. The measured low frequency half-wave voltage on the RF electrodes was typically 4.1 V. The S_{21} electro-optic response at 30 GHz in the Ka band was -4 dB. The corresponding effective half-wave voltage of 6.5 V is thus expected to reach the aim target of 6-7 V.

Fig.4 : Insertion loss variation (blue line) during temperature steps from -30°C up to +70°C

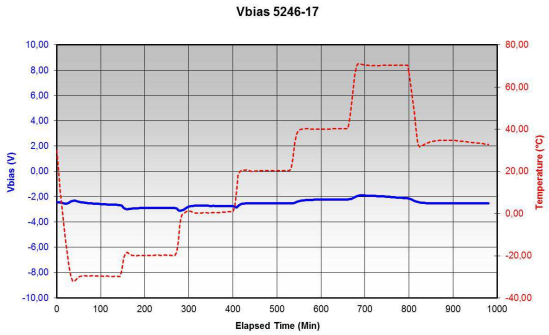

Fig.5 : DC bias drift (blue line) with temperature variations, from -30°C up to +70°C

The X-Cut and TI-WG devices showed optoelectronic results in compliance with the original target. Their high stability under temperature variations was also confirmed. The devices were hermetically sealed and submitted to 6 steps of temperature ranging from -30°C, -20°C, 0°C, 20°C, 40°C & 70°C. Each steps lasted 120 minutes. The insertion loss (IL) variations (Figure 4, blue line) and the bias voltage drift (Figure 5, blue line) were recorded and plotted for each of them, while the temperature variations are represented by a red dashed line..

The tested modulators exhibited a very high bias voltage stability over the whole temperature range, with peak to peak drift of 3 V for the worst case (1 V in the case of Fig. 5) while at stable temperature, the drift was very low. In all cases, the insertion loss remained stable (< 0.5 dB) over the whole temperature range.

Based on this optical modulator prototype dedicated to microwave photonic payloads, an evaluation based on space applications consideration was launched. Next paragraphs describe the adopted test plan.

IV. TEST PLAN

In order to fully assess the suitability of this new modulator design for the previously mentioned space applications, 8 identical samples were fabricated by Photline and evaluated through a functional and environmental test campaign. They were screened and then submitted to an initial characterisation. Two additional samples (#1946-12 & #1946-14) of similar technology (X-cut, Ti-WG) were used for irradiation (gamma & proton) tests.

The test plan sequence for the different samples is shown in table 2, and it can be summarised as follows:

- The sample (5246-18) was chosen as reference modulator and did not pass any of the tests. This sample was submitted to destructive physical analysis (DPA) at the end.
- The samples (#4816-11 & #6243-04) were submitted to mechanical tests only, i.e. SRS (Shock Response Spectrum), sine and random vibrations.
- The sample #4816-18 was submitted to the thermal vacuum test only (0°C 70°C).
- The samples #5246-17 was submitted to endurance test only (2000hrs)
- The sample #5246-06 was submitted to both mechanical tests and thermal vacuum tests.
- The sample #5246-13 was submitted to both thermal vacuum tests and endurance tests.
- The sample #5246-11 was submitted to the three sequences of mechanical tests, thermal vacuum tests and endurance tests then final DPA for comparison with the reference modulator #5246-18.

STEP	DESCRIPTION	SAMPLE #									
		4816-11	4816-18	5243-04	5246-06	5246-11	5246-13	5246-17	5246-18Ref	1946-12	1946-14
Production	Screening SCC 5000	T	T	T	T	T	T	T	T	T	T
Step 1	Initial Inspection	T	T	T	T	T	T	T	T	T	T
Step 2	Initial Optoelectronic Characterisation	T	T	T	T	T	T	T	T	T	T
Step 3	Irradiation γ									T	T
Step 4	Irradiation Proton									T	T
Step 5	Mechanical Test	T		T	T	T			R		
	Thermal vacuum Test		T		T	T	T		R		
Step 6	Endurance test					T	T	T	R		
Step 7	Final DPA					T			T		

Table 2. Test plan sequence and samples distribution (T: test, R: reference)

The initial and final characterisations were carried out by Thales Alenia Space, while intermediate characterisations were carried out by Alter Technology in collaboration with Universidad Politécnica de Madrid.

The measured characteristics were the following:

- Static E/O response, based on the output optical power measurement versus DC bias voltage (no RF signal applied). It provides optical insertion loss, DC Extinction Ratio and DC half wave voltage
- RF half-wave drive voltage ($V\pi_{RF}$) by optical power measurement at minimum transmission. The RF frequency signal is set at 30 GHz. 3rd-order interception point and RF voltage measurement ($V\pi_{RF}$) at 30 GHz based on the two-tone measurement method.
- Optical bandwidth, based on the output optical power measurement versus wavelength, at DC bias voltage (no RF signal applied) for maximum transmission at 1550 nm.

In next paragraphs, we report the results obtained on the different samples after each tests and we will check the main drift thus obtained. We focus in particular on the variations of the insertion loss and of the effective half wave drive voltage at 30 GHz, in order to conclude on the stability of the aimed FoM at the end of this space assessment.

V. TEST RESULTS

A. Irradiation test results

The irradiations tests were carried out in two steps. In the first step, modulators were exposed to gamma radiations with a cumulated dose up to 100 krad with intermediate characterisation and followed by thermal annealing steps. Table 3 summarizes the main variations of insertion loss and drive voltage. The second step was dedicated to proton radiations with doses up to 10^{10} p/cm^2. Table 3 summarizes the corresponding variations of drive voltage and insertion loss.

No major degradation of insertion loss (exceeding 1dB) and $V\pi_{RF}$ were observed after the two irradiation steps (gamma and proton) .

Parameters	Samples	10 krad	30 krad	60 krad	100 krad	annealing 24h	Annealing 168h	Annealing 70°C 168h	Proton $5x10^9$p/cm²	Proton $5x10^9$p/cm²	Proton $1x10^{10}$p/cm²
ΔIL(dB	1946-12	0.6	0.6	0.3	0.1	0.1	0.5	0.3	-0.03	-0.03	-0.05
	1946-14	-0.4	-1.2	-0.8	0.07	-0.6	-0.9	-1.0	-0.03	-0.01	-0.02
ΔVπ(V)	1946-12	-0.1	0.0	0.0	0.0	0.0	0.0	0.0	-0.17	-0.33	-0.75
	1946-14	-0.1	-0.2	-0.1	-0.1	-0.1	-0.1	-0.1	0.04	-0.02	-0.04

Table 3. IL and $V\pi_{RF}$ drifts of samples # 1846-12 and 1946-14
Gamma irradiation followed by thermal annealing steps, then Proton radiation

B. Overall test results

Fig. 6 shows the variations of the key parameters (Insertion loss IL and drive voltage $V\pi_{RF}$) measured after each main steps (mechanical shocks, sine vibrations, random vibration, thermal vacuum, endurance) with all intermediate characterisations.

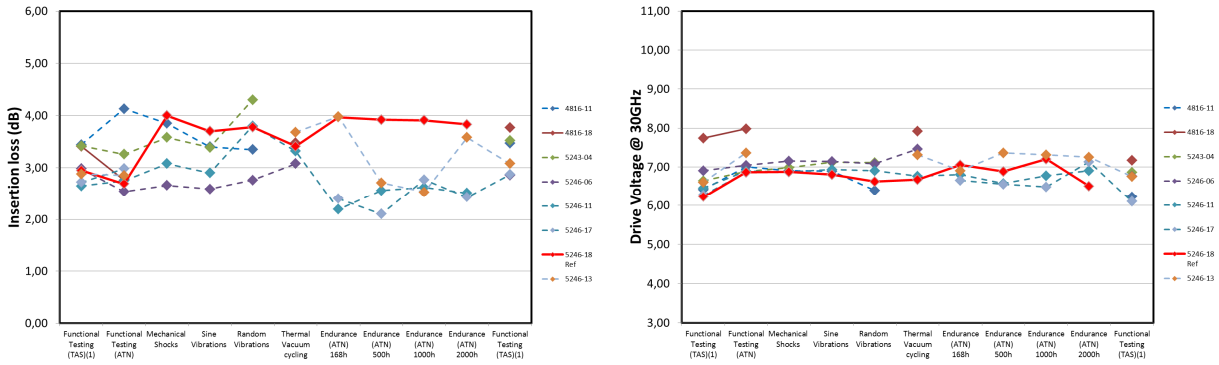

(a) (b)

Fig. 6 : Insertion loss IL (a) and drive voltage $V\pi_{RF}$ (b) drifts during tests achievements
(red line: reference modulator)

During the environmental test campaign no deleterious effect was observed. In particular, thermal and mechanical tests were successfully passed by the modulators tested: no dramatic variations of the main parameters (IL & $V\pi_{RF}$) were measured. However, thermal vacuum tests highlighted different behaviours among modulators submitted to this test possibly due to slight differences in the design. All samples were fully operational after the complete mechanical series, with very good stability on the DC Vπ and RF Vπ @30 GHz. Slight variation of IL parameter after random vibration could be observed on some samples.

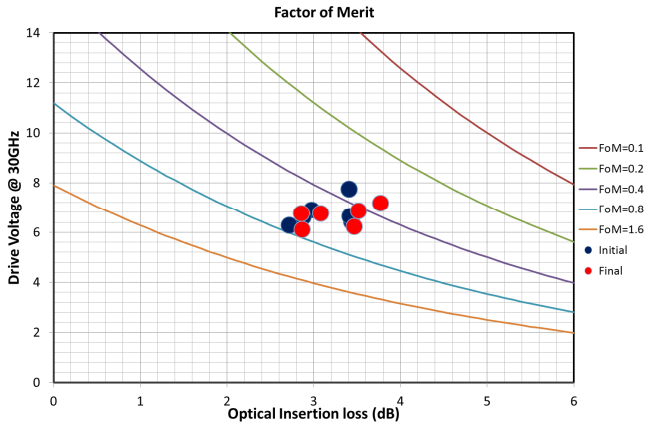

Fig. 7 **:** Figure of merit of the samples before (blue circles) and after (red circles) the tests campaign.

Following the environmental tests, a final functional test campaign was performed in order to evaluate the variations of the FoM defined in (1) between the beginning and the end of the full test campaign. The same

parameters as during the initial functional test were measured. Fig. 7 summarises the FoM variations of the samples on a chart taking into account both critical parameters (IL and $V\pi_{RF}$).

VI. CONCLUSION

The design of the modulators allowed reaching low insertion loss (2.6 dB at best) concurrently with relatively low driving voltage (6V). Thus, the reached figure of merit meets the requirements of photonic microwave payload in particular LO generation technique. The prototypes were submitted to a space assessment. The final characterisation showed no significant drift, in particular relative to insertion loss. The average insertion loss variation was found to be -0.12 dB while the average driving voltage drift was found to be -0.125 V when comparing the initial and final characterisations performed at 30 GHz.

This evaluation carried out on new multi GigaHertz optical modulators, anticipates a full space qualification process. The low drift of physical parameters after irradiation, vacuum thermal cycling in particular confirms the suitability of this technology of optical modulators to operate in space with a proven level of reliability within future microwave photonic payload.

ACKNOWLEDGEMENTS

This work was supported by the European Space Agency (ESA) under the ARTES 5 contract n°20101/06/NL/Sfe – Multi-Gigahertz Optical Modulator of Very Low RF Driving Power.

The author thank the European Space Agency and especially Nikos Karafolas, as technical officer of this activity, as well as national space agencies (CNES and INTA), for their support and collaboration during this project.

REFERENCES

[1] Edmond Chen and Antao Murphy, Editors. "Broadband Optical Modulators: Science, Technology, and Applications", CRC Press 2011,

[2] N. Dagli, "*Wide-Bandwidth Lasers and Modulators for RF Photonics*", IEEE Transactions on Microwave Theory and Techniques, vol 47, no. 7, july 1999, pp. 1151, 1171

[3] L.R. Dalton and W. H. Steier "*Electro-optic polymer modulators*" pp. 223-256. Broadband Optical Modulators: Science, Technology, and Applications. Ed. A. Chen and E. Murphy. CRC Press 2012

[5] C. Kazmierski, A. Konczykowska, F. Jorge, F. Blache, M. Riet, C. Jany, and A. Scavennec, "*100 Gb/s operation of an AlGaInAs semi-insulating buried heterojunction EML,*" in OFC 2009, San Diego, CA, paper OThT7, 2009. San Diego: IEEE

[6] S. R. Sakamoto, A. Jackson, and N. Dagli, "Substrate removed GaAs/AlGaAs electrooptic modulators," IEEE Photon. Technol. Lett., vol. 11, no. 10, pp. 1244-1246, Oct. 1999

[7] Tao Chu; Xi Xiao; Hao Xu; Xianyao Li; Zhiyong Li; Jinzhong Yu; Yude Yu, "High-speed silicon modulators,", 39th European Conference and Exhibition Optical Communication (ECOC 2013) 22-26 Sept. 2013,

[8] D. J. Thomson et al "Hi*gh Performance Mach–ZehnderBased Silicon Optical Modulators,*" Selected Topics in Quantum Electronics, IEEE Journal of , vol.19, no.6, pp.85,94, Nov.-Dec. 2013

[9] A. Le Kernec et al "Space Evaluation of Optical Modulators for Microwave Photonic On-Board Applications", International Conference on Space Optics, Rhodes, Greece, 4 – 8 October 2010.

[10] M. Sotom, B. Benazet, A. Le Kernec, M. Maignan "Microwave Photonic Technologies for Flexible Satellite Telecom Payloads" European Conference on Optical Communication, Sept. 20 – 24, 2009, Vienna, Austria.

[11] M. Aveline et al "Reconfigurable Microwave Photonic Repeater for Broadband Telecom Missions: Concepts and Technologies" International Conference on Space Optics, Oct. 7 – 10, 2014, Tenerife, Spain.